

# Status of the aligned two-Higgs-doublet model confronted with the Higgs data

Lei Wang, Xiao-Fang Han

*Department of Physics, Yantai University, Yantai 264005, PR China*

## Abstract

Imposing the theoretical constraints from vacuum stability, unitarity and perturbativity as well as the experimental constraints from the electroweak precision data, flavor observables and the non-observation of additional Higgs at collider, we study the implications of available Higgs signals on a two-Higgs-doublet model with the alignment of the down-type quarks and charged lepton Yukawa coupling matrices. Compared to the four traditional types of two-Higgs-doublet models, the model has two additional mixing angles  $\theta_d$  and  $\theta_l$  in the down-type quark and charged lepton Yukawa interactions. We find that the mixing angle  $\theta_d$  can loose the constraints on  $\sin(\beta - \alpha)$ ,  $\tan \beta$  and  $m_{H^\pm}$  sizably. The model can provide the marginally better fit to available Higgs signals data than SM, which requires the Higgs couplings with gauge bosons,  $u\bar{u}$  and  $d\bar{d}$  to be properly suppressed, and favors ( $1 < \theta_d < 2$ ,  $0.5 < \theta_l < 2.2$ ) for  $m_h = 125.5$  GeV and ( $0.5 < \theta_d < 2$ ,  $0.5 < \theta_l < 2.2$ ) for  $m_H = 125.5$  GeV. However, these Higgs couplings are allowed to have sizable deviations from SM for ( $m_h = 125.5$  GeV,  $125.5 \leq m_H \leq 128$  GeV) and ( $125$  GeV  $\leq m_h \leq 125.5$  GeV,  $m_H = 125.5$  GeV).

PACS numbers: 12.60.Fr, 14.80.Ec, 14.80.Bn

## I. INTRODUCTION

The CMS and ATLAS collaborations have announced the observation of a scalar around 125 GeV [1, 2], which is supported by the Tevatron search [3]. The properties of this particle with large experimental uncertainties are well consistent with the SM Higgs boson, which will give the strong constraints on the effects of new physics.

One of the simplest extension of the SM is obtained by adding a second  $SU(2)_L$  Higgs doublet [4]. The two-Higgs-doublet model (2HDM) has very rich Higgs phenomenology, including two neutral CP-even Higgs bosons  $h$  and  $H$ , one neutral pseudoscalar  $A$ , and two charged Higgs  $H^\pm$ . Further, the couplings of the CP-even Higgs bosons can deviate from SM Higgs boson sizably. Therefore, the observed signal strengths of the Higgs boson and the non-observation of additional Higgs can give the strong implications on the 2HDMs. The 2HDMs generically have tree-level flavor changing neutral currents (FCNC), which can be forbidden by a discrete symmetry. There are four types for 2HDMs, which are typically called the Type-I [5, 6], Type-II [5, 7], Lepton-specific, and Flipped models [8–13] according to their different Yukawa couplings. In light of the recent Higgs data, there have been various studies on these 2HDMs over the last few months [14–27].

In this paper, we focus on a two-Higgs-doublet model that allows both doublets to couple to the down-type quarks and charged leptons with aligned Yukawa matrices (A2HDM) [24, 28]. Also there is no tree-level FCNC in this model. Compared to the above four types of 2HDMs, there are two additional mixing angles in the Yukawa couplings of the down-type quarks and charged leptons. This model can be mapped to the four types of 2HDMs for the two angles are taken as specific values. There are also some works on the Higgs properties in the A2HDM after the discovery of Higgs boson [24, 25, 29–34]. After imposing the theoretical constraints from vacuum stability, unitarity and perturbativity as well as the experimental constraints from the electroweak precision data, flavor observables and the non-observation of additional Higgs at collider, we study the implication of the latest Higgs signals data on the A2HDM.

Our work is organized as follows. In Sec. II we recapitulate the A2HDM. In Sec. III we introduce the numerical calculations. In Sec. IV, we discuss the implications of the available Higgs signals on the A2HDM after imposing the theoretical and experimental constraints. Finally, we give our conclusion in Sec. V.

## II. ALIGNED TWO-HIGGS-DOUBLET MODEL

The general Higgs potential is written as [35]

$$\begin{aligned}
V = & m_{11}^2(\Phi_1^\dagger\Phi_1) + m_{22}^2(\Phi_2^\dagger\Phi_2) - \left[ m_{12}^2(\Phi_1^\dagger\Phi_2 + \text{h.c.}) \right] \\
& + \frac{\lambda_1}{2}(\Phi_1^\dagger\Phi_1)^2 + \frac{\lambda_2}{2}(\Phi_2^\dagger\Phi_2)^2 + \lambda_3(\Phi_1^\dagger\Phi_1)(\Phi_2^\dagger\Phi_2) + \lambda_4(\Phi_1^\dagger\Phi_2)(\Phi_2^\dagger\Phi_1) \\
& + \left[ \frac{\lambda_5}{2}(\Phi_1^\dagger\Phi_2)^2 + \text{h.c.} \right] + \left[ \lambda_6(\Phi_1^\dagger\Phi_1)(\Phi_1^\dagger\Phi_2) + \text{h.c.} \right] \\
& + \left[ \lambda_7(\Phi_2^\dagger\Phi_2)(\Phi_1^\dagger\Phi_2) + \text{h.c.} \right].
\end{aligned} \tag{1}$$

We focus on the CP-conserving model in which all  $\lambda_i$  and  $m_{12}^2$  are real. Further, we assume  $\lambda_6 = \lambda_7 = 0$ , which also facilitates the comparison to the four traditional types of 2HDMs. The two complex scalar doublets have the hypercharge  $Y = 1$ ,

$$\Phi_1 = \begin{pmatrix} \phi_1^+ \\ \frac{1}{\sqrt{2}}(v_1 + \phi_1^0 + ia_1) \end{pmatrix}, \quad \Phi_2 = \begin{pmatrix} \phi_2^+ \\ \frac{1}{\sqrt{2}}(v_2 + \phi_2^0 + ia_2) \end{pmatrix}. \tag{2}$$

Where  $v_1$  and  $v_2$  are the electroweak vacuum expectation values (VEVs) with  $v^2 = v_1^2 + v_2^2 = (246 \text{ GeV})^2$ . The ratio of the two VEVs is defined as usual to be  $\tan\beta = v_2/v_1$ . After spontaneous electroweak symmetry breaking, the physical scalars are two neutral CP-even  $h$  and  $H$ , one neutral pseudoscalar  $A$ , and two charged scalar  $H^\pm$ . These scalars are also predicted in the Higgs triplet models [36–38].

The Yukawa interactions of the Higgs doublets with the SM fermions can be given by

$$\begin{aligned}
-\mathcal{L} = & y_u \overline{Q}_L \tilde{\Phi}_2 u_R + y_d \overline{Q}_L (\cos\theta_d \Phi_1 + \sin\theta_d \Phi_2) d_R \\
& + y_l \overline{L}_L (\cos\theta_l \Phi_1 + \sin\theta_l \Phi_2) e_R + \text{h.c.},
\end{aligned} \tag{3}$$

where  $Q^T = (u_L, d_L)$ ,  $L^T = (\nu_L, l_L)$ , and  $\tilde{\Phi}_2 = i\tau_2\Phi_2^*$ .  $y_u$ ,  $y_d$  and  $y_l$  are  $3 \times 3$  matrices in family space.  $\theta_d$  and  $\theta_l$  parameterize the two Higgs doublets couplings to down-type quarks and charged leptons, respectively. Where a freedom is used to redefine the two linear combinations of  $\Phi_1$  and  $\Phi_2$  to eliminate the coupling of the up-type quarks to  $\Phi_1$  [24].

The tree-level couplings of the neutral Higgs bosons can have sizable deviations from those of SM Higgs boson. Table I shows the couplings of neutral Higgs bosons with respect to the SM Higgs boson. According to Table I, the A2HDM can be mapped to the four traditional types of 2HDMs via the angles  $\theta_d$  and  $\theta_l$  specified in Table II.

TABLE I: The tree-level couplings of the neutral Higgs bosons with respect to those of the SM Higgs boson.  $u$ ,  $d$  and  $l$  denote the up-type quarks, down-type quarks and the charged leptons, respectively. The angle  $\alpha$  parameterizes the mixing of two CP-even Higgses  $h$  and  $H$ .

	$VV$ ( $WW$ , $ZZ$ )	$u\bar{u}$	$d\bar{d}$	$l\bar{l}$
$h$	$\sin(\beta - \alpha)$	$\frac{\cos \alpha}{\sin \beta}$	$-\frac{\sin(\alpha - \theta_d)}{\cos(\beta - \theta_d)}$	$-\frac{\sin(\alpha - \theta_l)}{\cos(\beta - \theta_l)}$
$H$	$\cos(\beta - \alpha)$	$\frac{\sin \alpha}{\sin \beta}$	$\frac{\cos(\alpha - \theta_d)}{\cos(\beta - \theta_d)}$	$\frac{\cos(\alpha - \theta_l)}{\cos(\beta - \theta_l)}$
$A$	0	$-\frac{i}{\tan \beta} \gamma_5$	$-i \tan(\beta - \theta_d) \gamma_5$	$-i \tan(\beta - \theta_l) \gamma_5$

TABLE II: The values of mixing angles  $\theta_d$  and  $\theta_l$  for the four traditional types of 2HDMs.

	Type I	Type II	Lepton-specific	Flipped
$\theta_d$	$\frac{\pi}{2}$	0	$\frac{\pi}{2}$	0
$\theta_l$	$\frac{\pi}{2}$	0	0	$\frac{\pi}{2}$

### III. NUMERICAL CALCULATIONS

We have employed the following four codes to implement the various theoretical and experimental constraints. We require the A2HDM to explain the experimental data of flavor observables and the electroweak precision data within  $2\sigma$  range.

- **2HDMC-1.5** [39]: The code is used to implement the theoretical constraints from the vacuum stability, unitarity and coupling-constant perturbativity. Also the oblique parameters ( $S$ ,  $T$ ,  $U$ ) and  $\delta\rho$  are calculated and the corresponding experimental data are from [40].  $\delta\rho$  has been measured very precisely via Z-pole precision observables to be very close to 1, which imposes a strong constraint on the mass difference between the various Higgses in 2HDMs. In addition, the code 2HDMC-1.5 [83] which calculates the Higgs couplings and the decay branching fractions, provides the necessary inputs for the following three codes.
- **SuperIso-3.3** [41]: The code is used to implement the constraints from flavor observables, including  $B \rightarrow X_s \gamma$  [42],  $B_s \rightarrow \mu^+ \mu^-$  [43],  $B_u \rightarrow \tau \nu$  [44] and  $D_s \rightarrow \tau \nu$  [42]. Also the constraints from  $\Delta m_{B_d}$  [45] and  $\Delta m_{B_s}$  [45] are considered, which are calculated using the formulas in [46].

- **HiggsBounds-4.1.0** [47, 48]: The code is used to implement the exclusion constraints from the neutral and charged Higgses searches at LEP, Tevatron and LHC at 95% confidence level.
- **HiggsSignals-1.1.0** [49, 50]: The code is used to perform a global  $\chi^2$  fit to the most up-to-date signal strength measurements as of November 2013. We consider the 73 Higgs signal strengths observables from ATLAS [51–59], CMS [60–72], CDF [73] and D0 [74] collaborations as well as the four Higgs mass measurements from the ATLAS and CMS  $h \rightarrow \gamma\gamma$  and  $h \rightarrow ZZ^* \rightarrow 4l$  analyses, which are listed in the [50]. In our discussions, we will pay particular attention to the surviving samples with  $\chi^2 - \chi_{\min}^2 \leq 6.18$ , where  $\chi_{\min}^2$  denotes the minimum  $\chi^2$ . These samples correspond to the 95% confidence level regions in any two dimensional plane of the model parameters when explaining the Higgs data (corresponding to be within  $2\sigma$  range).

In our calculations, the inputs parameters are taken as  $m_{12}^2$ , the physical Higgs masses ( $m_h, m_H, m_A, m_{H^\pm}$ ), the vacuum expectation value ratio ( $\tan \beta$ ), the CP-even Higgs mixing angle ( $\alpha$ ), and the mixing angles of the down-type quark and charge lepton Yukawa couplings ( $\theta_d, \theta_l$ ). We fix respectively  $m_h$  and  $m_H$  as 125.5 GeV, and scan randomly the parameters in the following ranges:

$$\begin{aligned}
& 50 \text{ GeV} \leq m_A, m_{H^\pm} \leq 900 \text{ GeV}, \\
& -1 \leq \sin(\beta - \alpha) \leq 1, \quad 0.1 \leq \tan \beta \leq 50, \\
& 0 \leq \theta_d \leq \pi, \quad 0 \leq \theta_l \leq \pi, \\
& m_{12}^2 \text{ (GeV}^2\text{)} = \pm(0.1)^2, \pm(1)^2, \pm(5)^2, \pm(10)^2, \pm(30)^2, \pm(50)^2, \\
& \quad \pm(100)^2, \pm(180)^2, \pm(300)^2, \pm(400)^2, \pm(500)^2, \\
& \text{Scenario A : } m_h = 125.5 \text{ GeV}, \quad 125.5 \text{ GeV} \leq m_H \leq 900 \text{ GeV}, \\
& \text{Scenario B : } m_H = 125.5 \text{ GeV}, \quad 20 \text{ GeV} \leq m_h \leq 125.5 \text{ GeV}.
\end{aligned} \tag{4}$$

HiggsSignals-1.1.0 automatically consider the effects of any neutral Higgs boson on  $\chi^2$  if its mass satisfies

$$|m_{h_i} - \hat{m}_s| \leq \Delta \hat{m}_s. \tag{5}$$

Where  $h_i$  denotes  $h, H$  and  $A$ .  $\hat{m}_s$  is the mass of signal  $s$  and  $\Delta \hat{m}_s$  is the experimental mass resolution of the analysis associated to signal  $s$ . However, if the  $\chi^2$  contribution from the

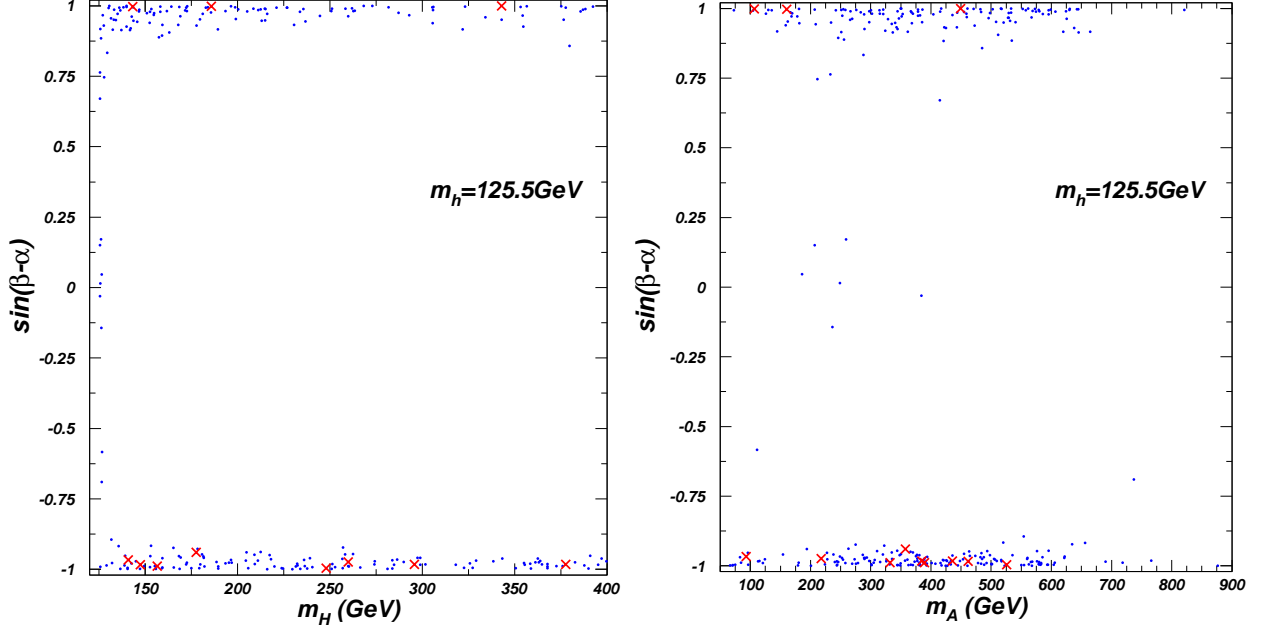


FIG. 1: The scatter plots of surviving samples in scenario A projected on the planes of  $\sin(\beta - \alpha)$  versus  $m_H$  and  $\sin(\beta - \alpha)$  versus  $m_A$ . The crosses (red), and bullets (blue) samples respectively have the values of  $\chi^2$  in the ranges of  $81.0 \sim 82.2$  and  $82.2 \sim 87.2$ , where the three values are respectively the minimal value of  $\chi^2$  in scenario A ( $\chi^2_{Amin}$ ), the SM value ( $\chi^2_{SM}$ ) and the value of  $\chi^2$  at  $2\sigma$  level in scenario A ( $\chi^2_{A2\sigma}$ ).

measured Higgs mass is activated, the combinations with a Higgs boson mass which does not fulfill Eq. (5) are still considered. For the detailed introduction on the calculation of  $\chi^2$ , see [49, 50].

## IV. RESULTS AND DISCUSSIONS

### A. Scenario A

Let us begin by discussing the scenario A in which the mass of the light CP-even Higgs  $h$  is fixed as 125.5 GeV. In Fig. 1, we project the surviving samples with  $\chi^2$  being within  $2\sigma$  range on the planes of  $\sin(\beta - \alpha)$  versus  $m_H$  and  $\sin(\beta - \alpha)$  versus  $m_A$ , respectively. The left panel shows that, for the heavy CP-even Higgs mass is close to 125.5 GeV, it can give the important contributions to  $\chi^2$ , and the absolute values of  $\sin(\beta - \alpha)$  can be allowed to

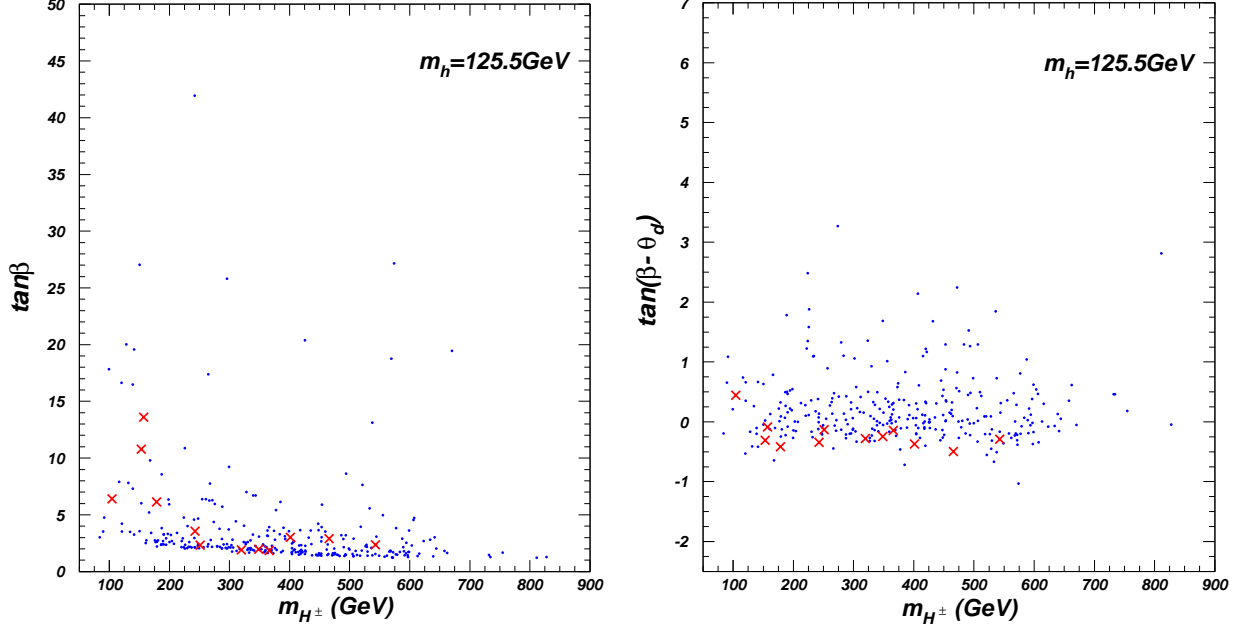


FIG. 2: Same as Fig. 1, but projected on the planes of  $\tan \beta$  versus  $m_{H^\pm}$  and  $\tan(\beta - \theta_d)$  versus  $m_{H^\pm}$ .

be as low as 0, in which the  $HVV$  couplings approach to SM while  $hVV$  approach to 0. For  $m_H \geq 128$  GeV,  $\sin(\beta - \alpha)$  is allowed to be in the ranges of  $0.83 \sim 1$  and  $-1 \sim -0.89$ . A small value of  $\chi^2$  favors a large absolute value of  $\sin(\beta - \alpha)$ , which denotes that the absolute values of  $hVV$  couplings approach to SM.

Unlike the heavy CP-even Higgs, the right panel of Fig. 1 shows that the CP-odd Higgs  $A$  does not give the very visible effects on  $\chi^2$  around 125.5 GeV compared to the other mass ranges.  $m_A$  is required to be larger than 63 GeV, and the on-shell decay  $h \rightarrow AA$  is kinematically forbidden, which hardly affects the observed Higgs signals.

In Fig. 2, the surviving samples are projected on the planes of  $\tan \beta$  versus  $m_{H^\pm}$  and  $\tan(\beta - \alpha)$  versus  $m_{H^\pm}$ . The left panel shows that the surviving samples favor  $1 < \tan \beta < 5$  and allow  $\tan \beta > 30$  for  $m_{H^\pm} > 230$  GeV. The constraints from  $\Delta m_{B_d}$  and  $\Delta m_{B_s}$  require  $\tan \beta$  to be larger than 1 for the whole range of  $m_{H^\pm}$ , and larger than 3 for  $m_{H^\pm} < 100$  GeV. The right panel shows that the surviving samples favor  $-0.5 < \tan(\beta - \theta_d) < 0.5$ . The flavor interactions mediated by  $H^\pm$  are proportional to  $\tan(\beta - \theta_d)$ . The constraints from the flavor observables allow  $m_{H^\pm}$  to be smaller than 100 GeV for the very small absolute of  $\tan(\beta - \theta_d)$ , and  $\tan(\beta - \theta_d)$  to be larger than 3 for  $m_{H^\pm} > 250$  GeV. In addition, the samples with smaller  $\chi^2$  than SM favor  $\tan(\beta - \theta_d)$  to be in the range of  $-0.5 \sim 0$  for  $m_{H^\pm} > 150$

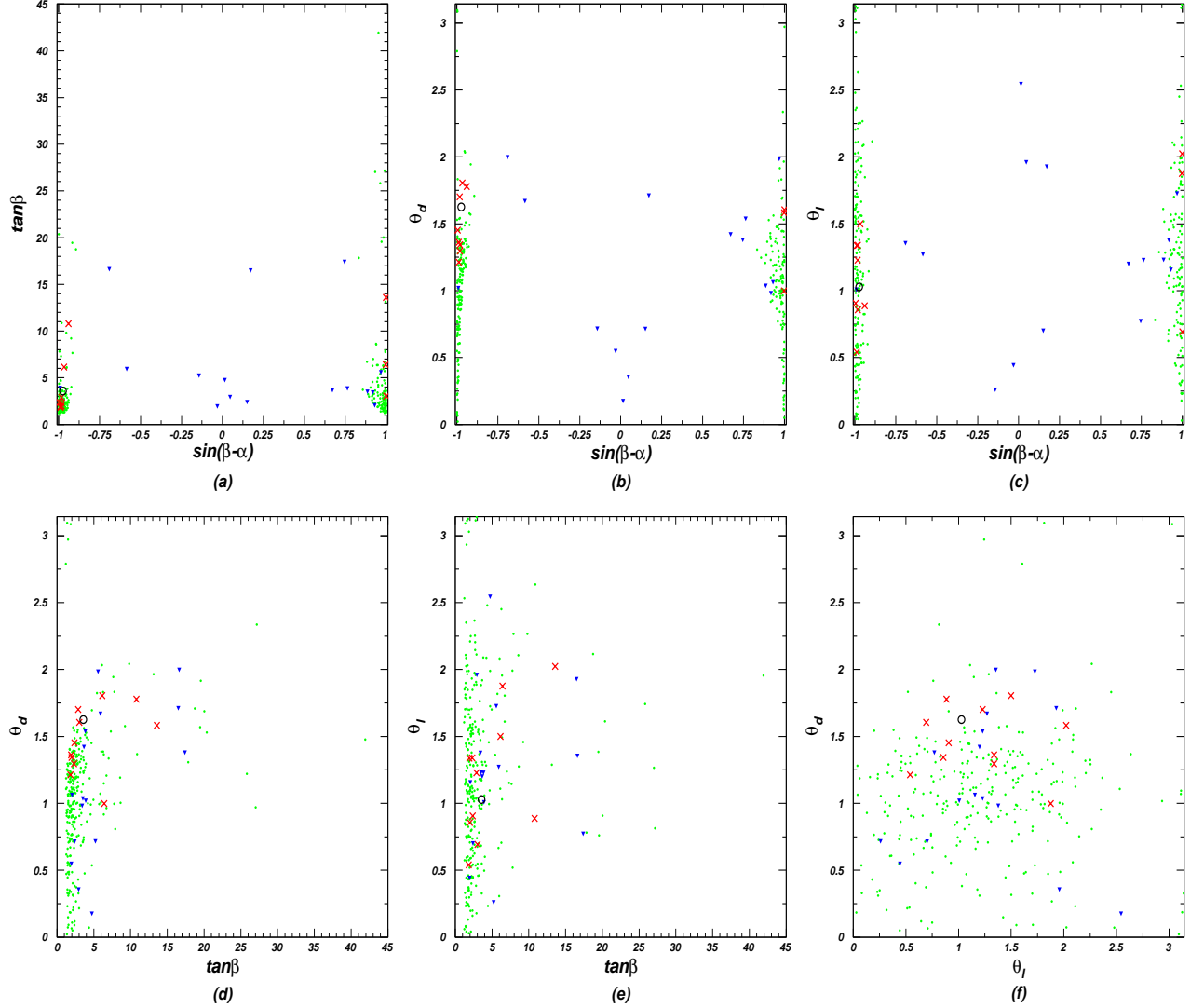


FIG. 3: The scatter plots of surviving samples in scenario A projected on the planes of mixing angles. The  $\chi^2$  values of the crosses (red), bullets (green) and inverted triangles (blue) samples are respectively in the ranges of  $\chi_{Amin}^2 \sim \chi_{SM}^2$  and  $\chi_{SM}^2 \sim \chi_{A2\sigma}^2$  for  $128 \text{ GeV} \leq m_H \leq 900 \text{ GeV}$ , and  $\chi_{SM}^2 \sim \chi_{A2\sigma}^2$  for  $125.5 \text{ GeV} \leq m_H < 128 \text{ GeV}$ . The  $\chi^2$  values of the circle (black) is  $\chi_{Amin}^2$ .

GeV.

The contributions of the heavy CP-even Higgs boson to  $\chi^2$  can be sizably suppressed for  $m_H \geq 128 \text{ GeV}$ . Therefore, we classify the surviving samples into groups:  $125.5 \text{ GeV} \leq m_H < 128 \text{ GeV}$  and  $128 \text{ GeV} \leq m_H \leq 900 \text{ GeV}$ . In Fig. 3, the two groups of surviving samples are projected on the planes of mixing angles ( $\sin(\beta - \alpha)$ ,  $\tan \beta$ ,  $\theta_d$  and  $\theta_l$ ). Fig. 3 (a) shows that  $\tan \beta$  can be over 20 for  $\sin(\beta - \alpha)$  is close to 1. Fig. 3 (b) shows that, for  $m_H > 128 \text{ GeV}$ , the mixing angle  $\theta_d$  can loose constraints on  $\sin(\beta - \alpha)$  visibly. For example, for



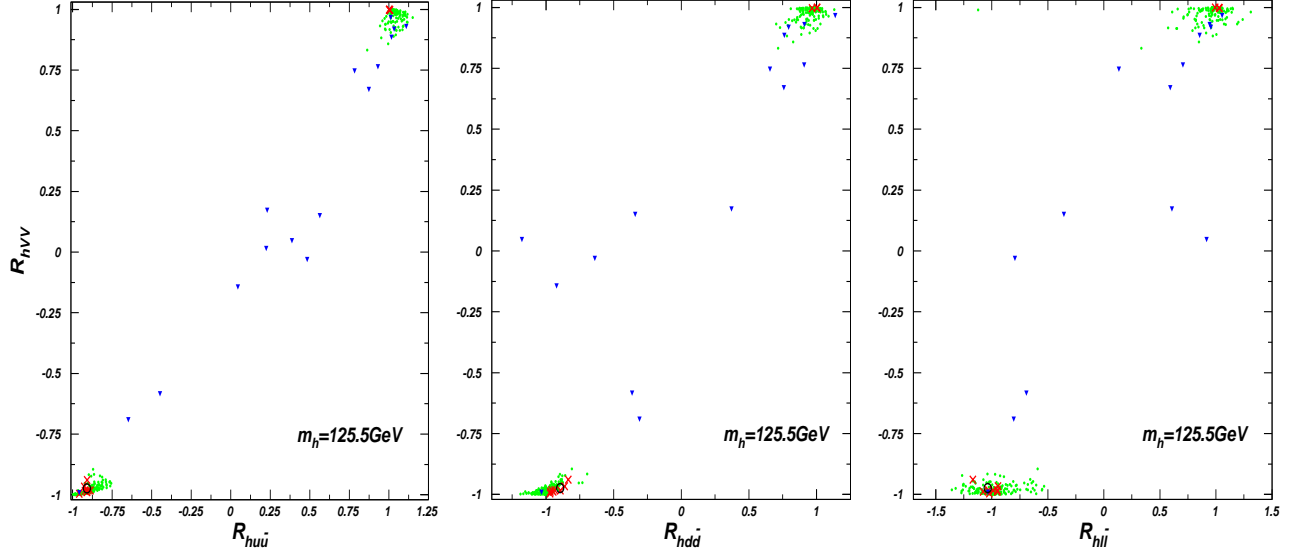


FIG. 4: Same as Fig. 3, but projected on the planes of  $R_{hVV}$  versus  $R_{hu\bar{u}}$ ,  $R_{hVV}$  versus  $R_{hd\bar{d}}$  and  $R_{hVV}$  versus  $R_{hl\bar{l}}$ .  $R_{hVV}$  and  $R_{hf\bar{f}}$  denote the light CP-even Higgs couplings to gauge bosons and  $f\bar{f}$  ( $f = u, d, l$ ) normalized to the SM couplings, respectively.

$\theta_d \simeq 0$  (Type-II and Flipped 2HDMs), the absolute value of  $\sin(\beta - \alpha)$  is required to be very close to 1. While  $\sin(\beta - \alpha)$  are allowed to vary in the range of  $0.83 \sim 1$  and  $-1 \sim -0.89$  for  $\theta_d$  has the properly large value. Also Fig. 3 (c) shows that  $\sin(\beta - \alpha)$  in the positive range is required to be very close to 1 for  $\theta_l \simeq 0$  (Type-II and Lepton-specific 2HDMs).

According to Figs. 3 (d) and (e), although the surviving samples favor a small value of  $\tan\beta$ , the value of  $\chi^2$  can be smaller than SM for a large  $\tan\beta$  when  $\theta_d$  and  $\theta_l$  have the proper large values, such as  $\tan\beta = 13.5$ ,  $\theta_d = 1.6$  and  $\theta_l = 2.0$ .

Fig. 3 (f) shows that the samples with smaller  $\chi^2$  than SM are favored in the range of  $1 < \theta_d < 2$  and  $0.5 < \theta_l < 2.2$ . Thus, it is possible that Type-I 2HDM gives the smaller value of  $\chi^2$  than SM. The minimal value of  $\chi^2$  (81.0) appears at  $\theta_d = 1.7$  and  $\theta_l = 1.3$ .

In Fig. 4, the surviving samples are projected on the planes of Higgs couplings. For  $125.5 \text{ GeV} \leq m_H < 128 \text{ GeV}$ , the heavy CP-even Higgs gives the important contributions to  $\chi^2$ . Therefore, there may be sizable deviations from SM for the couplings  $hV\bar{V}$ ,  $hu\bar{u}$ ,  $hd\bar{d}$  and  $hl\bar{l}$ . For  $m_H \geq 128 \text{ GeV}$  and the  $hV\bar{V}$  coupling with the small absolute value, the  $hb\bar{b}$  coupling by suppressed properly is required to obtain enough large  $Br(h \rightarrow ZZ^*)$  and  $Br(h \rightarrow \gamma\gamma)$ . The  $h \rightarrow \gamma\gamma$  and  $h \rightarrow ZZ^* \rightarrow 4l$  have the rather precise measurements and mass resolution, which play a very important role in the calculations of  $\chi^2$ . The signal

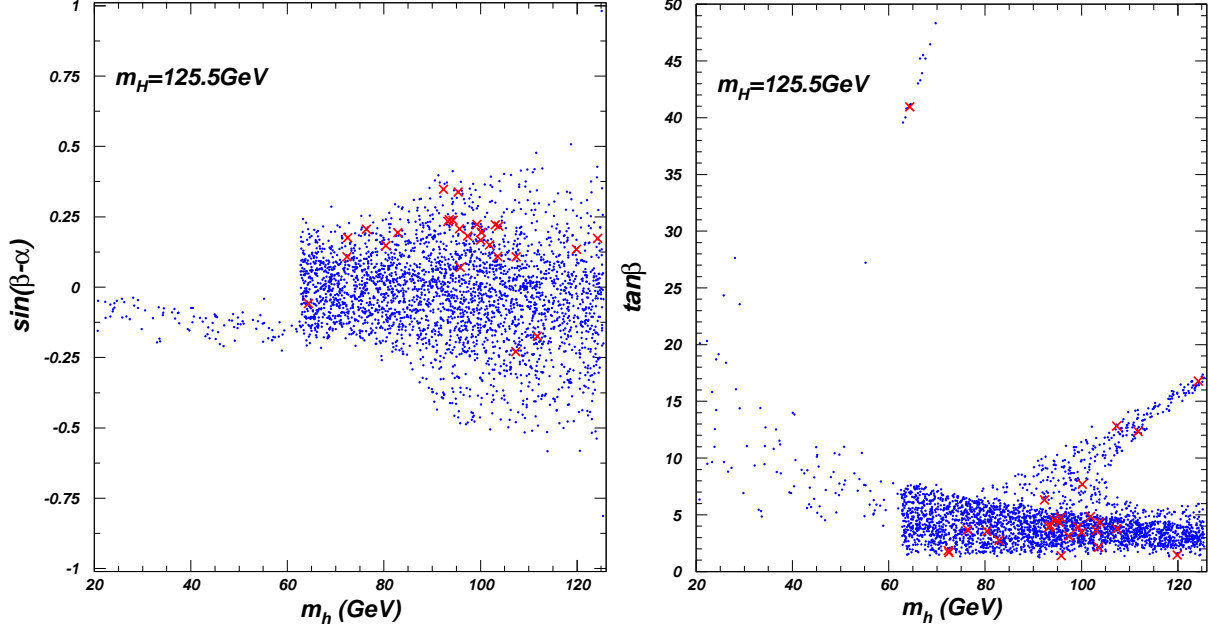


FIG. 5: The scatter plots of surviving samples in scenario B projected on the planes of  $\sin(\beta - \alpha)$  versus  $m_h$  and  $\tan \beta$  versus  $m_h$ . The crosses (red) and bullets (blue) samples respectively have the values of  $\chi^2$  in the ranges of  $81.5 \sim 82.2$  and  $82.2 \sim 87.7$ , where the three values are respectively the minimal value of  $\chi^2$  in scenario B ( $\chi_{Bmin}^2$ ), the SM value ( $\chi_{SM}^2$ ) and the value of  $\chi^2$  at  $2\sigma$  level in scenario B ( $\chi_{B2\sigma}^2$ ).

strengths of  $h \rightarrow \tau\tau$  have a large uncertainty and the signals are not important in the calculations of  $\chi^2$ . In addition, the mass resolution of  $h \rightarrow \tau\tau$  is 20 GeV for the analysis of ATLAS [56, 57] and 25 GeV for CMS [68], CDF [73] and D0 [74]. Therefore,  $H$  and  $A$  with  $100 \sim 150$  GeV may contribute to  $\chi^2$ . The constraints on  $h\tau\bar{\tau}$  is much more weakened than  $hu\bar{u}$  and  $hd\bar{d}$ .

For the samples with smaller  $\chi^2$  than SM, there is the same sign for the light CP-even Higgs couplings to fermions and gauge bosons. Compared to SM, the  $hVV$ ,  $hu\bar{u}$  and  $hd\bar{d}$  couplings are suppressed, and the suppressions are allowed to be as low as 0.94, 0.90 and 0.83, while the absolute value of  $R_{hll}$  are allowed to be as high as 1.2.

## B. Scenario B

Now we discuss the scenario B in which the mass of the heavy CP-even Higgs  $H$  is fixed as 125.5 GeV. In Fig. 5, we project the surviving samples with  $\chi^2$  being within  $2\sigma$  range on

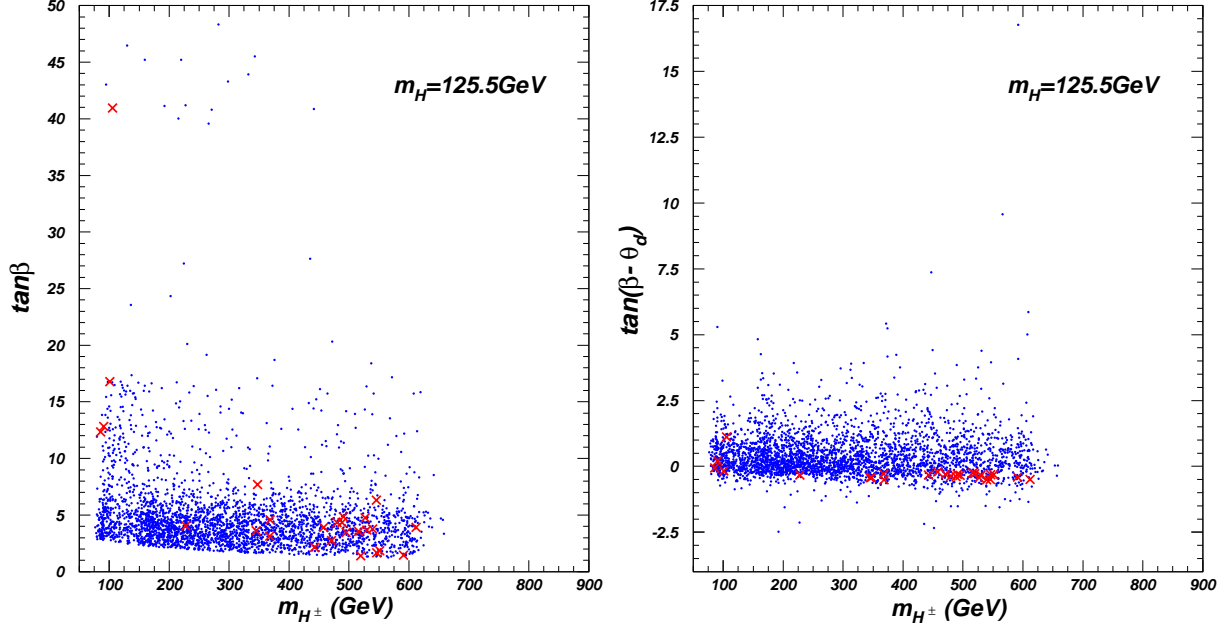


FIG. 6: Same as Fig. 5, but projected on the planes of  $\tan \beta$  versus  $m_{H^\pm}$  and  $\tan(\beta - \theta_d)$  versus  $m_{H^\pm}$ .

the planes of  $\sin(\beta - \alpha)$  versus  $m_h$  and  $\tan \beta$  versus  $m_h$ , respectively. The left panel shows that, for  $125 \text{ GeV} \leq m_h \leq 125.5 \text{ GeV}$ , the absolute values of  $\sin(\beta - \alpha)$  can be allowed to be as high as 1, which denotes  $hVV$  couplings approach to SM while  $HVV$  approach to 0. Such light CP-even Higgs can give the important contributions to  $\chi^2$ . The minimal absolute value of  $\sin(\beta - \alpha)$  decreases with  $m_h$  in principle. The light CP-even Higgs can be allowed to be as low as 20 GeV for  $-0.25 < \sin(\beta - \alpha) \leq 0$ . To be consistent with LEP constraints, the suppression of  $h\bar{b}b$  coupling is also required for some surviving samples in addition to the small absolute value of  $\sin(\beta - \alpha)$ . In addition, the small values of  $\chi^2$  favor  $-0.25 < \sin(\beta - \alpha) < 0.38$ , which denotes that the absolute values of  $HVV$  couplings are close to SM. The right panel shows that  $\tan \beta$  is required to be larger than 4 for  $m_h < 60 \text{ GeV}$ , which is due to the constraints of the observed Higgs signals on the opening decay  $H \rightarrow hh$ .

In Fig. 6, the surviving samples are projected on the planes of  $\tan \beta$  versus  $m_{H^\pm}$  and  $\tan(\beta - \theta_d)$  versus  $m_{H^\pm}$ . The left panel shows that the surviving samples favor  $1 < \tan \beta < 7$  and allow  $\tan \beta > 40$  for the proper  $m_{H^\pm}$ . Similar to scenario A,  $\tan \beta$  is required to be larger than 1 for the whole range of  $m_{H^\pm}$ , and larger than 3 for the  $m_{H^\pm} < 100 \text{ GeV}$ . The right panel shows that the surviving samples favor  $-1 < \tan(\beta - \theta_d) < 2.5$ . The constraints

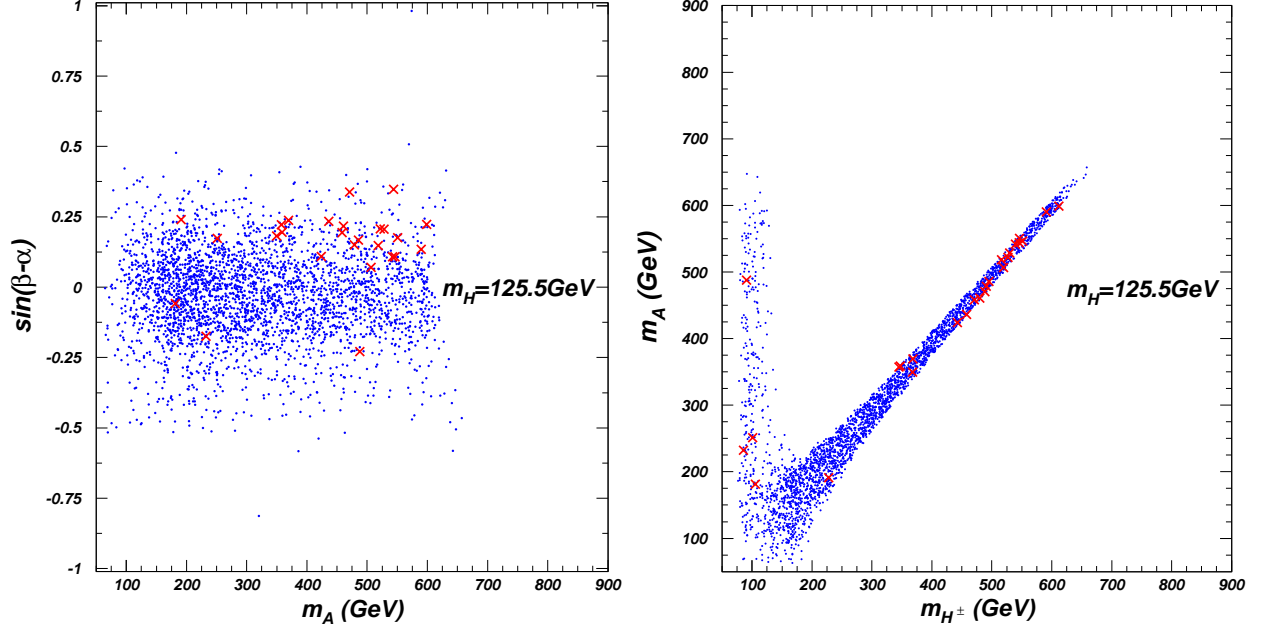


FIG. 7: Same as Fig. 5, but projected on the planes of  $\sin(\beta - \alpha)$  versus  $m_A$  and  $m_A$  versus  $m_{H^\pm}$ .

from the flavor observables require the absolute value of  $\tan(\beta - \theta_d)$  to be smaller than 2.5 for  $m_{H^\pm} < 100$  GeV, and allow  $\tan(\beta - \theta_d)$  to be larger than 10 for  $m_{H^\pm} > 600$  GeV. The samples with smaller  $\chi^2$  than SM favor  $\tan(\beta - \theta_d)$  to be in the range of  $-0.5 \sim 0$  for the large  $m_{H^\pm}$  and be enhanced for  $m_{H^\pm}$  around 100 GeV.

In Fig. 7, the surviving samples are projected on the planes of  $\sin(\beta - \alpha)$  versus  $m_A$  and  $m_A$  versus  $m_{H^\pm}$ . Similar to scenario A, the CP-odd Higgs  $A$  does not give the very visible effects on the  $\chi^2$  around 125.5 GeV compared to the other mass ranges. The on-shell decay  $H \rightarrow AA$  is kinematically forbidden, which hardly affects the observed Higgs signals. The right panel shows that most of samples lie in the region where there is small mass difference between  $m_A$  and  $m_{H^\pm}$ , and some other samples lie in the small region where  $m_{H^\pm}$  is around 100 GeV and has large mass difference from  $m_A$ . Assuming  $m_{12}^2 = 0$ , Baradhwaj Coleppa et al. have shown the strong correlations between  $m_A$  and  $m_{H^\pm}$  in the Type-II 2HDM [16]. Here  $m_{12}^2$  is taken as various values, the strong correlations still exist but the latter region becomes slightly wider than [16]. The main reason is from the constraints of  $\Delta\rho$ , which is also studied in detail in [75]. Since there is small mass difference between  $m_h$  and  $m_H$  for the scenario B,  $m_A$  and  $m_{H^\pm}$  should have the small mass difference to cancel the contributions of  $m_h$  and  $m_H$  to  $\Delta\rho$ . However, for  $m_{H^\pm}$  is around  $m_H$ , the contributions to  $\Delta\rho$  from  $(m_h, m_{H^\pm})$  and  $(m_A, m_{H^\pm})$  loops can be canceled by the  $(m_h, m_H)$  and  $(m_A, m_H)$  loops.

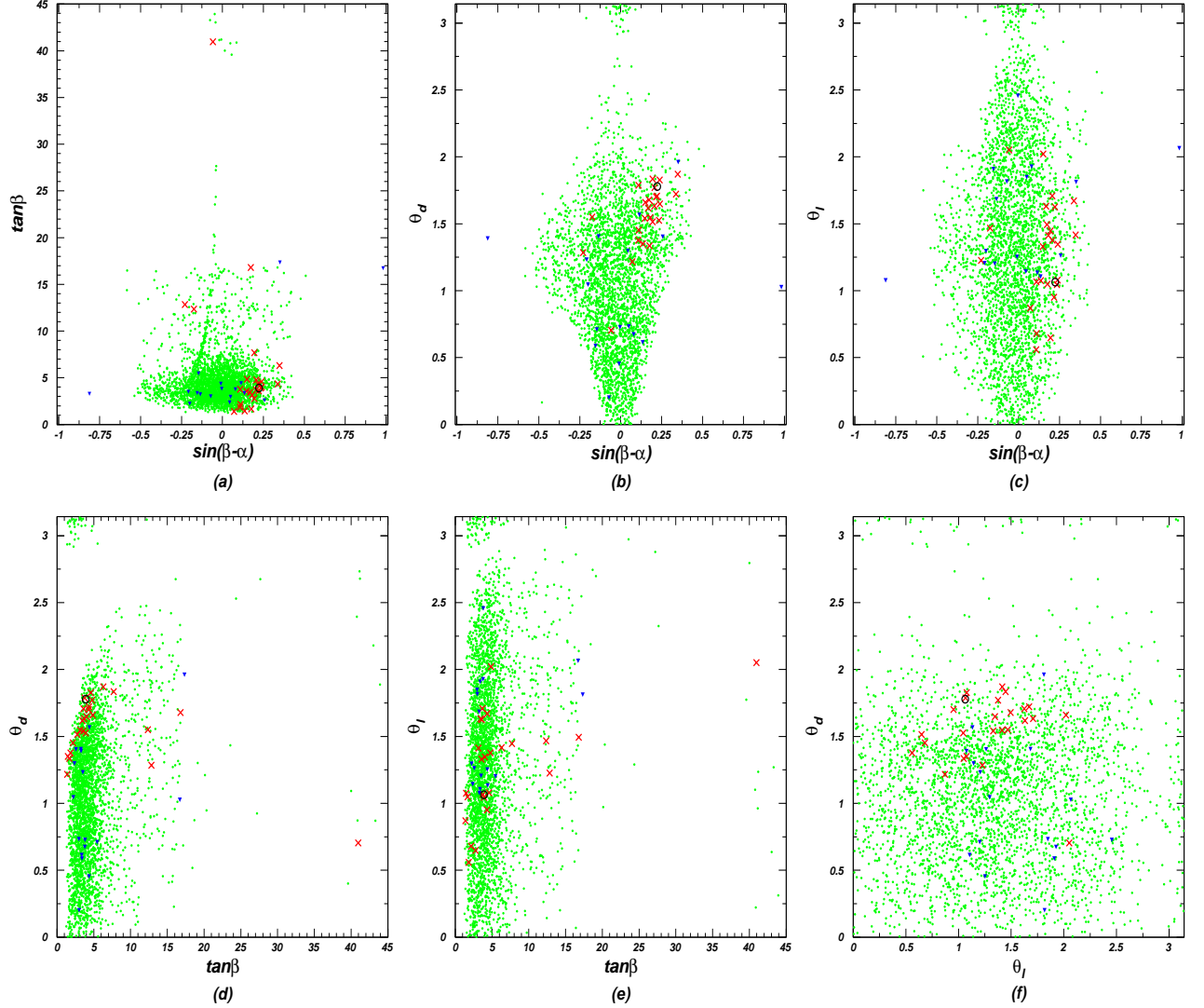


FIG. 8: The scatter plots of surviving samples in scenario B projected on the planes of mixing angles. The  $\chi^2$  values of the crosses (red), bullets (green) and inverted triangles (blue) samples are respectively in the ranges of  $\chi_{Bmin}^2 \sim \chi_{SM}^2$  and  $\chi_{SM}^2 \sim \chi_{B2\sigma}^2$  for  $20 \text{ GeV} \leq m_H < 125 \text{ GeV}$ , and  $\chi_{SM}^2 \sim \chi_{B2\sigma}^2$  for  $125 \text{ GeV} \leq m_H < 125.5 \text{ GeV}$ . The  $\chi^2$  values of the circle (black) is  $\chi_{Bmin}^2$ .

Thus  $m_A$  is allowed to vary from 70 GeV to 700 GeV for  $m_{H^\pm}$  around 100 GeV.

The contributions of the light CP-even Higgs boson to  $\chi^2$  can be sizably suppressed for  $m_h < 125 \text{ GeV}$ . Therefore, we classify the surviving samples into groups:  $20 \text{ GeV} \leq m_H < 125 \text{ GeV}$  and  $125 \text{ GeV} \leq m_H \leq 125.5 \text{ GeV}$ . In Fig. 8, the two groups of surviving samples are projected on the planes of mixing angles. Fig. 8 (a) shows that the samples with  $\tan \beta > 20$  require  $\sin(\beta - \alpha)$  to approach to 0. Fig. 8 (b) shows that, for  $m_h < 125 \text{ GeV}$ ,  $\theta_d$  can loose the constraints on  $\sin(\beta - \alpha)$  sizably. For example, for  $\theta_d \simeq 0$  (Type-II and Flipped

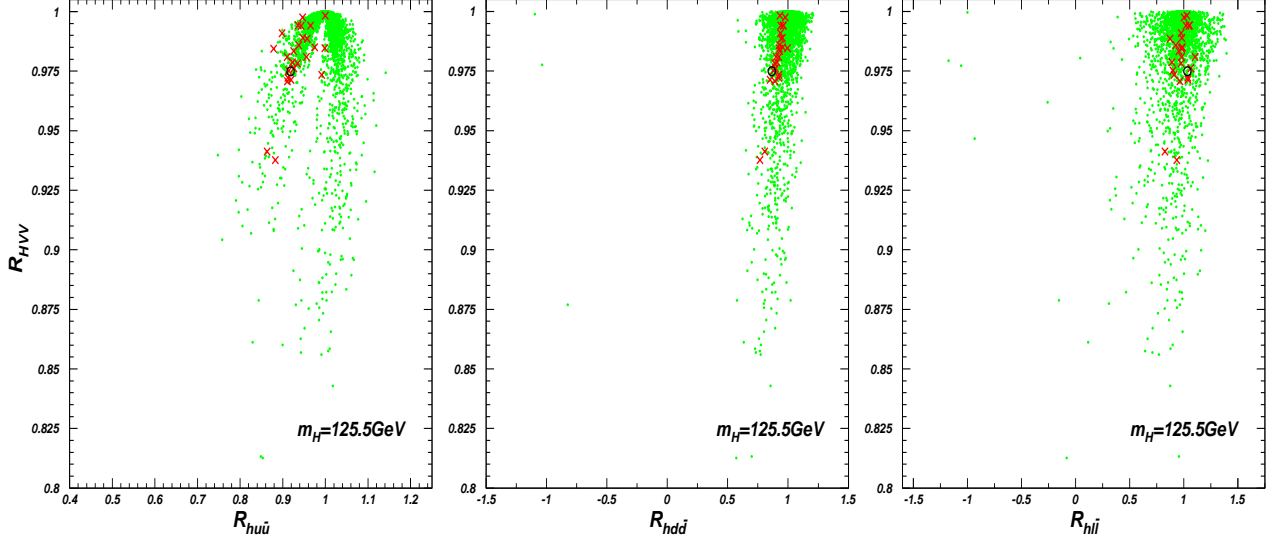


FIG. 9: Same as Fig. 8, but only the samples with  $20 \text{ GeV} \leq m_h < 120 \text{ GeV}$  projected on the planes of  $R_{HV V}$  versus  $R_{Hu\bar{u}}$ ,  $R_{HV V}$  versus  $R_{Hd\bar{d}}$  and  $R_{HV V}$  versus  $R_{Hl\bar{l}}$ .  $R_{HV V}$  and  $R_{Hf\bar{f}}$  denote the heavy CP-even Higgs couplings to gauge bosons and  $f\bar{f}$  ( $f = u, d, l$ ) normalized to the SM couplings, respectively.

2HDMs),  $\sin(\beta - \alpha)$  is allowed to vary from -0.1 to 0.06. While for  $\theta_d \simeq \frac{\pi}{2}$  (Type-I and Lepton-specific 2HDMs),  $\sin(\beta - \alpha)$  is allowed to vary in the range of  $-0.5 \sim 0.44$ . Further, Fig. 8 (c) shows that  $\theta_l \simeq 0$  (Type-II and Lepton-specific 2HDMs) also gives the strong constraints on  $\sin(\beta - \alpha)$ ,  $-0.18 \leq \sin(\beta - \alpha) \leq 0.12$ .

Similar to scenario A, Figs. 8 (d) and (e) show that, although the surviving samples favor  $1 < \tan \beta < 7$ , the value of  $\chi^2$  can be smaller than SM for a large  $\tan \beta$  when  $\theta_d$  and  $\theta_l$  have the proper large values. Even for  $\tan \beta = 41$ , the value of  $\chi^2$  can be smaller than SM for  $\theta_d = 0.7$  and  $\theta_l = 2.1$ . Fig. 8 (f) shows that the samples with smaller than SM are in the range of  $0.5 < \theta_d < 2$  and  $0.5 < \theta_l < 2.2$ . The minimal value of  $\chi^2$  (81.5) appears at  $\theta_d = 1.8$  and  $\theta_l = 1.1$ .

In Fig. 9, the surviving samples with  $20 \text{ GeV} \leq m_h < 125 \text{ GeV}$  are projected on the planes of Higgs couplings. Similar to scenario A, for the  $HV V$  coupling with the small absolute value, the  $Hb\bar{b}$  coupling by suppressed properly is required to obtain enough large  $Br(h \rightarrow ZZ^*)$  and  $Br(h \rightarrow \gamma\gamma)$ . The constraints on  $h\tau\bar{\tau}$  is much more weaken than  $hu\bar{u}$  and  $hdd$ . For the samples with smaller  $\chi^2$  than SM, there is the same sign for the heavy CP-even Higgs couplings to fermions and gauge bosons. Compared to SM, the  $HV V$ ,  $Hu\bar{u}$  and  $Hd\bar{d}$

TABLE III: The detailed information of the four samples with the minimal values of  $\chi^2$  in the scenario A ( $125.5 \text{ GeV} \leq m_H < 128 \text{ GeV}$  and  $128 \text{ GeV} \leq m_H \leq 900 \text{ GeV}$ ) and scenario B ( $20 \text{ GeV} \leq m_h < 125 \text{ GeV}$  and  $125 \text{ GeV} \leq m_h \leq 125.5 \text{ GeV}$ ). Where  $R_{Au\bar{u}}$ ,  $R_{Ad\bar{d}}$  and  $R_{Al\bar{l}}$  are from the interactions,  $\frac{m_f}{v} R_{Af\bar{f}} A \bar{f} \gamma^5 f$  with  $f = u, d, l$ .

	scenario A	scenario A	scenario B	scenario B
$m_h$ (GeV)	125.5	125.5	99.3	125.4
$m_H$ (GeV)	126.1	259.9	125.5	125.5
$m_A$ (GeV)	258.9	217.4	598.8	342.3
$m_{H^\pm}$ (GeV)	139.1	242.8	612.1	347.1
$m_{12}^2$ (GeV)	900	10000	0.01	900
$\sin(\beta - \alpha)$	0.172	-0.973	0.222	-0.042
$\tan \beta$	16.48	3.57	3.91	17.07
$\theta_d$	1.71	1.63	1.78	1.53
$\theta_l$	1.93	1.03	1.06	1.30
$\chi^2$	83.3	81.0	81.5	83.0
$R_{hVV}$	0.172	-0.973	0.222	-0.042
$R_{hu\bar{u}}$	0.231	-0.909	0.472	0.016
$R_{hd\bar{d}}$	0.371	-0.895	0.702	-0.020
$R_{hl\bar{l}}$	0.608	-1.04	-0.033	-0.260
$R_{HVV}$	0.985	0.229	0.975	0.999
$R_{Hu\bar{u}}$	0.975	0.502	0.918	1.002
$R_{Hd\bar{d}}$	0.950	0.561	0.866	1.000
$R_{Hl\bar{l}}$	0.909	-0.040	1.033	0.990
$R_{Au\bar{u}}$	-0.061	-0.280	-0.256	-0.059
$R_{Ad\bar{d}}$	0.202	0.341	0.491	0.022
$R_{Al\bar{l}}$	0.443	-0.277	-0.262	-0.217

couplings are suppressed, and the suppressions are allowed to be as low as 0.94, 0.86 and 0.77, respectively. However, the  $Hl\bar{l}$  coupling can be allowed to have a 10% enhancement, or 17% suppression.

In Table III we present the detailed information for the four samples with the minimal

values of  $\chi^2$  in the scenario A ( $125.5 \text{ GeV} \leq m_H < 128 \text{ GeV}$  and  $128 \text{ GeV} \leq m_H \leq 900 \text{ GeV}$ ) and scenario B ( $20 \text{ GeV} \leq m_h < 125 \text{ GeV}$  and  $125 \text{ GeV} \leq m_h \leq 125.5 \text{ GeV}$ ). For the four cases,  $\theta_d$  and  $\theta_l$  of the samples with the minimal  $\chi^2$  are in the ranges of  $1.5 \sim 1.8$  and  $1.0 \sim 2.0$ . For the scenario A with  $128 \text{ GeV} \leq m_H \leq 900 \text{ GeV}$  and scenario B with  $20 \text{ GeV} \leq m_h < 125 \text{ GeV}$ , the absolute values for the  $125.5 \text{ GeV}$  Higgs couplings to  $VV$  approach to SM, and the couplings to  $u\bar{u}$  and  $d\bar{d}$  have around 10% suppressions compared to SM. The minimal  $\chi^2$  values of the two cases are respectively 81.0 and 81.5, which are marginally smaller than SM value (82.2). This implies that the A2HDM can provide marginally better fit to the observed Higgs signals than SM at the expense of additional parameters. Similarly, the minimal dilaton model can not provide much better fit to LHC and Tevatron Higgs data than SM [76]. The fit given by little Higgs models at most approaches to SM for very large scale  $f$  [77–79], while Next-to-Minimal Supersymmetric Standard Model [80–82] can give much better fit than SM.

After Moriond 2013, the CMS diphoton data has changed drastically, which is no longer enhanced. In addition to the four typical 2HDMs, the Higgs data after Moriond 2013 have been used to examine the A2HDM in Refs. [24, 25, 31, 33]. Refs. [33] assumes the both Higgs doublet fields ( $\Phi_1$  and  $\Phi_2$ ) to couple to the up-type quarks, down-type quarks and charged leptons with aligned Yukawa matrices. However, Refs. [24, 25, 31] and this paper use a freedom to eliminate the coupling of up-type quarks to  $\Phi_1$ . In our discussions, we consider more relevant theoretical and experimental constraints than Refs. [24, 25, 31]. Our paper shows that the theoretical constraint from perturbativity disfavors a large  $\tan\beta$  much more visibly than Ref. [25]. In our analysis, we consider the 73 Higgs signal strengths observables from ATLAS, CMS, CDF and D0 collaborations as well as the four Higgs mass measurements from ATLAS and CMS, which are more than Refs. [24, 25, 31]. The **HiggsSignals-1.1.0** is employed to take into account the signal efficiencies, experimental mass resolution and uncertainties. Our paper shows that the Higgs couplings to gauge bosons and fermions are not more strongly constrained than Refs. [24, 25, 31, 33]. Refs. [24, 31] focus on the constraints of the Higgs signals on the Higgs couplings to gauge bosons and fermions. In addition to these Higgs couplings, we also give the allowed parameters spaces in detail, including  $\tan\beta$ ,  $\sin(\beta - \alpha)$ ,  $\theta_d$ ,  $\theta_l$ , the neutral and charged Higgs masses, and show explicitly that the proper  $\theta_d$  can loose the constraints on  $\sin(\beta - \alpha)$ ,  $\tan\beta$  and  $m_{H^\pm}$  sizably. An interesting finding is that when  $\theta_d$  and  $\theta_l$  have the proper large values, the value of  $\chi^2$  can



be smaller than SM for a large  $\tan\beta$  (even  $\tan\beta = 41$ ), although the  $2\sigma$  Higgs data and the relevant theoretical and experimental constraints favor a small  $\tan\beta$ .

## V. CONCLUSION

In this note, we studied the implications of the latest Higgs signals on a two-Higgs-doublet model with the alignment of the down-type quarks and charged lepton Yukawa coupling matrices. In our analysis, we consider the theoretical constraints from vacuum stability, unitarity and perturbativity as well as the experimental constraints from the electroweak precision data, flavor observables and the non-observation of additional Higgs at collider. We obtained the following observations:

(i) In the scenario A ( $m_h$  is fixed as 125.5 GeV),  $\sin(\beta - \alpha)$  is allowed to be in the range of  $-1 \sim 1$  for  $125.5 \text{ GeV} \leq m_H < 128 \text{ GeV}$ . For  $m_H \geq 128 \text{ GeV}$ ,  $\sin(\beta - \alpha)$  is allowed to be in the ranges of  $0.83 \sim 1$  and  $-1 \sim -0.89$  for the proper  $\theta_d$ , but be very close to 1 or -1 for  $\theta_d = 0$ . Also, the mixing angle  $\theta_d$  can loose the constraints on  $\tan\beta$  and  $m_{H^\pm}$  sizably. Although the surviving samples favor  $1 < \tan\beta < 5$ , the value of  $\chi^2$  can be smaller than SM for a large  $\tan\beta$  when  $\theta_d$  and  $\theta_l$  have the proper large values.  $m_{H^\pm}$  is allowed to be below 100 GeV for the absolute value of  $\tan(\beta - \theta_d)$  is very small, and the samples with the smaller  $\chi^2$  than SM favor  $0.5 < \tan(\beta - \theta_d) < 0$  for  $m_{H^\pm} > 150 \text{ GeV}$ .

(ii) In the scenario B ( $m_H$  is fixed as 125.5 GeV),  $\sin(\beta - \alpha)$  is allowed to be in the range of  $-1 \sim 1$  for  $125 \text{ GeV} \leq m_h \leq 125.5 \text{ GeV}$ , and the minimal absolute value of  $\sin(\beta - \alpha)$  decreases with  $m_h$  in principle. The light CP-even Higgs can be allowed to be as low as 20 GeV for  $-0.25 < \sin(\beta - \alpha) \leq 0$ . The constraints of the observed Higgs signals on the opening decay  $H \rightarrow hh$  require  $\tan\beta$  to be larger than 4 for  $m_h < 60 \text{ GeV}$ . Similar to scenario A, the mixing angle  $\theta_d$  can loose the constraints on  $\sin(\beta - \alpha)$ ,  $\tan\beta$  and  $m_{H^\pm}$  sizably. For  $m_h < 125 \text{ GeV}$ ,  $\theta_d$  around  $\frac{\pi}{2}$  can allow  $\sin(\beta - \alpha)$  to be in the range of  $-0.5 \sim 0.44$ . Although the surviving samples favor  $1 < \tan\beta < 7$ , the value of  $\chi^2$  can be smaller than SM for  $\tan\beta > 40$  when  $\theta_d$  and  $\theta_l$  have the proper large values.  $m_{H^\pm}$  is allowed to be below 100 GeV for the absolute value of  $\tan(\beta - \theta_d)$  is smaller than 2.5, and the samples with the smaller  $\chi^2$  than SM favor  $-0.5 < \tan(\beta - \theta_d) < 0$  for the large  $m_{H^\pm}$ .

(iii) The model can provide the marginally better fit to available Higgs signals data than SM. For  $m_h = 125.5 \text{ GeV}$ , the absolute values of  $hVV$ ,  $hw\bar{u}$  and  $hdd$  couplings are

respectively allowed to be as low as 0.94, 0.90 and 0.83, and  $\theta_d$  and  $\theta_l$  are favored in the ranges of  $1 \sim 2$  and  $0.5 \sim 2.2$ . For  $m_H = 125.5$  GeV, the  $HVV$ ,  $Hu\bar{u}$  and  $Hd\bar{d}$  couplings are respectively allowed to be as low as 0.94, 0.86 and 0.77, and  $\theta_d$  and  $\theta_l$  are favored in the ranges of  $0.5 \sim 2$  and  $0.5 \sim 2.2$ .

### Acknowledgment

We would like to thank Nazila Mahmoudi, Johan Rathsman and Oscar Stål for helpful discussions on the codes SuperIso, 2HDMC and HiggsBounds. This work was supported by the National Natural Science Foundation of China (NNSFC) under grant Nos. 11005089, 11105116 and 11175151.

- 
- [1] S. Chatrchyan et al. [CMS Collaboration], Phys. Lett. B **716**, 30 (2012).
  - [2] G. Aad et al. [ATLAS Collaboration], Phys. Lett. B **716**, 1 (2012).
  - [3] T. Aaltonen *et al.* [CDF and D0 Collaborations], Phys. Rev. D **88**, 052014 (2013).
  - [4] T. D. Lee, Phys. Rev. D **8**, 1226 (1973).
  - [5] H. E. Haber, G. L. Kane and T. Sterling, Nucl. Phys. B **161**, 493 (1979).
  - [6] L. J. Hall and M. B. Wise, Nucl. Phys. B **187**, 397 (1981).
  - [7] J. F. Donoghue and L. F. Li, Phys. Rev. D **19**, 945 (1979).
  - [8] V. D. Barger, J. L. Hewett and R. J. N. Phillips, Phys. Rev. D **41**, 3421 (1990).
  - [9] Y. Grossman, Nucl. Phys. B **426**, 3 (1994).
  - [10] A. G. Akeroyd and W. J. Stirling, Nucl. Phys. B **447**, 3 (1995).
  - [11] A. G. Akeroyd, Phys. Lett. B **377**, 95 (1996).
  - [12] A. G. Akeroyd, J. Phys. G **24**, 1983 (1998).
  - [13] M. Aoki, S. Kanemura, K. Tsumura and K. Yagyu, Phys. Rev. D **80**, 015017 (2009).
  - [14] C. -Y. Chen and S. Dawson, Phys. Rev. D **87**, 055016 (2013).
  - [15] B. Grinstein and P. Uttayarat, JHEP **1306**, 094 (2013) [Erratum-ibid. 1309, 110 (2013)].
  - [16] B. Coleppa, F. Kling, S. Su, arXiv:1305.0002
  - [17] O. Eberhardt, U. Nierste, M. Wiebusch, JHEP **07**, 118 (2013).
  - [18] C. -W. Chiang and K. Yagyu, JHEP **1307**, 160 (2013).

- [19] B. Grinstein and P. Uttayarat, JHEP **1306**, 094 (2013).
- [20] C. -Y. Chen, S. Dawson and M. Sher, Phys. Rev. D **88**, 015018 (2013).
- [21] L. Wang, X.-F. Han, JHEP **1205**, 088 (2012).
- [22] N. Craig, J. Galloway and S. Thomas, arXiv:1305.2424.
- [23] G. Belanger, B. Dumont, U. Ellwanger, J. F. Gunion and S. Kraml, Phys. Rev. D **88**, 075008 (2013).
- [24] V. Barger, L. L. Everett, H. E. Logan and G. Shaughnessy, arXiv:1308.0052.
- [25] D. Lopez-Val, T. Plehn and M. Rauch, JHEP **1310**, 134 (2013).
- [26] S. Choi, S. Jung and P. Ko, JHEP **1310**, 225 (2013).
- [27] S. Chang, S. K. Kang, J. -P. Lee, K. Y. Lee, S. C. Park and J. Song, arXiv:1310.3374.
- [28] A. Pich, P. Tuzon, Phys. Rev. D **80**, 091702 (2009).
- [29] W. Altmannshofer, S. Gori and G. D. Kribs, Phys. Rev. D **86**, 115009 (2012).
- [30] Y. Bai, V. Barger, L. L. Everett and G. Shaughnessy, Phys. Rev. D **87**, 115013 (2013).
- [31] K. Cheung, J. S. Lee, P.-Y. Tseng, arXiv:1310.3937.
- [32] A. Celis, V. Ilisie, A. Pich, JHEP **1307**, 053 (2013).
- [33] A. Celis, V. Ilisie, A. Pich, arXiv:1310.7941.
- [34] W. Altmannshofer, S. Gori, G. D. Kribs, Phys. Rev. D **86**, 115009 (2012).
- [35] R. A. Battye, G. D. Brawn, A. Pilaftsis, JHEP **1108**, 020 (2011).
- [36] W. Konetschny, W. Kummer, Phys. Lett. B **70**, 433 (1977).
- [37] T. P. Cheng, L. F. Li, Phys. Rev. D **22**, 2860 (1980).
- [38] L. Wang, X.-F. Han, Phys. Rev. D **87**, 015015 (2013).
- [39] D. Eriksson, J. Rathsmann, O. Stål, Comput. Phys. Commun. **181**, 189-205 (2010); Comput. Phys. Commun. **181**, 833-834 (2010).
- [40] J. Beringer *et al.* (Particle Data Group), Phys. Rev. D **86**, 010001 (2012).
- [41] F. Mahmoudi, Comput. Phys. Commun. **180**, 1579-1673 (2009).
- [42] Y. Amhis *et al.* [Heavy Flavor Averaging Group], arXiv:1207.1158
- [43] R. Aaij *et al.* [LHCb Collaboration], Phys. Rev. Lett. **110**, 021801 (2013).
- [44] <http://www.slac.stanford.edu/xorg/hfag/rare/2013/radll/index.html>
- [45] Particle Data Group, 2013 partial update for the 2014 edition.
- [46] C. Q. Geng and J. N. Ng, Phys. Rev. D **38**, 2857 (1988) [Erratum-ibid. D 41, 1715 (1990)].
- [47] P. Bechtle, O. Brein, S. Heinemeyer, G. Weiglein, K. E. Williams, Comput. Phys. Commun.

- 181**, 138-167 (2010).
- [48] P. Bechtle, O. Brein, S. Heinemeyer, O. Stål, T. Stefaniak, G. Weiglein, K. E. Williams, arXiv:1311.0055.
  - [49] P. Bechtle, S. Heinemeyer, O. Stål, T. Stefaniak, G. Weiglein, arXiv:1305.1933.
  - [50] P. Bechtle, S. Heinemeyer, O. Stål, T. Stefaniak, G. Weiglein, "HiggsSignals-1.1 release note", see "[http://higgsbounds.hepforge.org/HS-1.1\\_releasenote.pdf](http://higgsbounds.hepforge.org/HS-1.1_releasenote.pdf)."
  - [51] ATLAS Collaboration, ATLAS-CONF-2013-030.
  - [52] G. Aad *et al.* [ATLAS Collaboration], Phys. Lett. B **726**, 88-119 (2013).
  - [53] ATLAS Collaboration, ATLAS-CONF-2013-013.
  - [54] ATLAS Collaboration, ATLAS-CONF-2012-091.
  - [55] ATLAS Collaboration, ATLAS-CONF-2013-012.
  - [56] ATLAS Collaboration, ATLAS-CONF-2013-034.
  - [57] ATLAS Collaboration, ATLAS-CONF-2012-160.
  - [58] ATLAS collaboration, ATLAS-CONF-2013-079; ATLAS-COM-CONF-2013-080.
  - [59] ATLAS collaboration, ATLAS-CONF-2013-075; ATLAS-COM-CONF-2013-069.
  - [60] CMS Collaboration, CMS-PAS-HIG-13-003.
  - [61] CMS Collaboration, CMS-PAS-HIG-13-022.
  - [62] CMS Collaboration, CMS-PAS-HIG-13-017.
  - [63] CMS Collaboration, CMS-PAS-HIG-13-009.
  - [64] CMS Collaboration, CMS-PAS-HIG-13-002.
  - [65] CMS Collaboration, CMS-PAS-HIG-12-015.
  - [66] CMS Collaboration, CMS-PAS-HIG-13-001.
  - [67] CMS Collaboration, CMS-PAS-HIG-13-007.
  - [68] CMS Collaboration, CMS-PAS-HIG-13-004.
  - [69] CMS Collaboration, CMS-PAS-HIG-13-012.
  - [70] CMS Collaboration, CMS-PAS-HIG-13-020.
  - [71] CMS Collaboration, CMS-PAS-HIG-13-019.
  - [72] CMS Collaboration, CMS-PAS-HIG-13-015.
  - [73] T. Aaltonen *et al.* [CDF Collaboration], Phys. Rev. D **88**, 052013 (2013).
  - [74] V. M. Abazov *et al.* [D0 Collaboration], Phys. Rev. D **88**, 052011 (2013).
  - [75] E. Cervero and J.-M. Gerard, Phys. Lett. B **712**, 255 (2012).

- [76] J. Cao, Y. He, P. Wu, M. Zhang, J. Zhu, arXiv:1311.6661.
- [77] L. Wang, J. M. Yang, J. Zhu, Phys. Rev. D **88**, 075018 (2013).
- [78] X.-F. Han, L. Wang, J. M. Yang, J. Zhu, Phys. Rev. D **87**, 055004 (2013).
- [79] J. Reuter, M. Tonini, JHEP **0213**, 077 (2013).
- [80] J. Cao, Z. Heng, J. M. Yang, J. Zhu, JHEP **1210**, 079 (2012).
- [81] J.-J. Cao, Z.-X. Heng, J. M. Yang, Y.-M. Zhang, J.-Y. Zhu, JHEP **1203**, 086 (2012).
- [82] J. F. Gunion, Y. Jiang, S. Kraml, Phys. Lett. B **710**, 454-459 (2012).
- [83] A bug is modified:  $\Gamma(h \rightarrow Z\gamma) = 0$  for  $m_h < m_Z$ .